AFCRL-71-0455
19 AUGUST 1971
ENVIRONMENTAL RESEARCH PAPERS, NO. 371

AIR FORCE CAMBRIDGE RESEARCH LABORATORIES
L. G. HANSCOM FIELD, BEDFORD, MASSACHUSETTS

Atmospheric Optics Measurements With a Balloon-Borne Nephelometer

FRANK W. GIBSON
FRANK K. DEARBORN

AIR FORCE SYSTEMS COMMAND
United States Air Force

Unclassified
Security Classification

DOCUMENT CONTROL DATA - R&D

(Security classification of title, body of abstract and indexing annotation must be entered when the overall report is classified)

1. ORIGINATING ACTIVITY *(Corporate author)*
Air Force Cambridge Research Laboratories (OP)
L.G. Hanscom Field
Bedford, Massachusetts 01730

2a. REPORT SECURITY CLASSIFICATION
Unclassified

2b. GROUP

3. REPORT TITLE
ATMOSPHERIC OPTICS MEASUREMENTS WITH A BALLOON-BORNE NEPHELOMETER

4. DESCRIPTIVE NOTES *(Type of report and inclusive dates)*
Scientific. Interim.

5. AUTHOR(S) *(First name, middle initial, last name)*
Frank W. Gibson
Frank K. Dearborn

6. REPORT DATE	7a. TOTAL NO. OF PAGES	7b. NO. OF REFS
19 August 1971	30	16

8a. CONTRACT OR GRANT NO.	9a. ORIGINATOR'S REPORT NUMBER(S)
b. PROJECT, TASK, WORK UNIT NOS. 7621-04-01	AFCRL-71-0455
c. DOD ELEMENT 62101F	9b. OTHER REPORT NO(S) *(Any other numbers that may be assigned this report)*
d. DOD SUBELEMENT 681000	ERP No. 371

10. DISTRIBUTION STATEMENT
Approved for public release; distribution unlimited.

11. SUPPLEMENTARY NOTES	12. SPONSORING MILITARY ACTIVITY
TECH, OTHER	Air Force Cambridge Research Laboratories (OP) L.G. Hanscom Field Bedford, Massachusetts 01730

13. ABSTRACT

A large modified polar nephelometer was constructed for the purpose of making high altitude atmospheric optics measurements. The instrument is balloon-borne and measures the angular volume scattering function from ground to better than 26 km in absolute quantities. The results of the initial flight with the unit are presented and they depict the variability in this parameter over the altitude profile for three scattering angles and four wavelengths. In addition, the polarization and the forward-to-backscatter ratio of the scattered light are shown to be sensitive indicators of the atmosphere's vertical aerosol structure. The import of these preliminary results is, however, in pointing out the capabilities of this instrument, which can provide quantitative information on fundamental optical parameters of the atmosphere without the constraints inherent in other techniques.

DD FORM 1 NOV 65 1473

Unclassified
Security Classification

Unclassified

Security Classification

14. KEY WORDS	LINK A		LINK B		LINK C	
	ROLE	WT	ROLE	WT	ROLE	WT
Light scattering Nephelometer Angular volume scattering function Degree of polarization Forward-to-backscatter ratio Aerosol scattering in troposphere and stratosphere						

Unclassified

Security Classification

AFCRL-71-0455
19 AUGUST 1971
ENVIRONMENTAL RESEARCH PAPERS, NO. 371

OPTICAL PHYSICS LABORATORY PROJECT 7621
AIR FORCE CAMBRIDGE RESEARCH LABORATORIES
L. G. HANSCOM FIELD, BEDFORD, MASSACHUSETTS

Atmospheric Optics Measurements With a Balloon-Borne Nephelometer

FRANK W. GIBSON
FRANK K. DEARBORN

AIR FORCE SYSTEMS COMMAND
United States Air Force

Abstract

A large modified polar nephelometer was constructed for the purpose of making high altitude atmospheric optics measurements. The instrument is balloon-borne and measures the angular volume scattering function from ground to better than 26 km in absolute quantities. The results of the initial flight with the unit are presented and they depict the variability in this parameter over the altitude profile for three scattering angles and four wavelengths. In addition, the polarization and the forward-to-backscatter ratio of the scattered light are shown to be sensitive indicators of the atmosphere's vertical aerosol structure. The import of these preliminary results is, however, in pointing out the capabilities of this instrument, which can provide quantitative information on fundamental optical parameters of the atmosphere without the constraints inherent in other techniques.

Contents

Illustrations

Illustrations

Atmospheric Optics Measurements With a Balloon-Borne Nephelometer

1. INTRODUCTION

Experimental investigations of altitude variations in the optical scattering properties of the atmosphere usually involve measurements of the extinction coefficient or the angular volume scattering function, $\beta(\phi)$. The latter quantity is the more difficult to measure accurately as it represents the amount of light an irradiated volume element sends out in a particular direction. This places stringent requirements on the measurement apparatus, if reliable results are to be obtained, since the angular distribution of the scattered light as well as its wavelength and polarization depend on sundry properties of the air molecules and aerosols contained in the volume element. These properties include molecular and aerosol number densities, size distribution, refractive index, and particle shape. In situ measurements of $\beta(\phi)$ to high altitudes thus provide information on fundamental atmospheric parameters and their variability with altitude.

Generally, methods for measuring $\beta(\phi)$ have used natural or artificial light sources. With the sun as the source, the luminance of the horizon in various azimuths is observed or the sky radiance is measured in the sun's vertical. Moreover, the sky radiance at an inclination to the sun's vertical provides a direct measurement of the scattering function for the entire atmosphere, from which the altitude dependence can be determined under certain conditions (Bullrich, 1964).

(Received for publication 18 August 1971)

However, these radiance measurements involve integrating the total atmospheric light path, which renders the results unreliable, primarily because of multiple scattering effects.

More accurate data have been obtained with artificial sources such as searchlights or nephelometers. Although searchlight and laser radar techniques (Elterman, 1966; Collins and Ligda, 1966; Clemesha et al, 1967; Grams and Fiocco, 1967) provide good profiles of the extinction or attenuation coefficients as a function of altitude, the volume scattering function can be ascertained explicitly for only a limited range of backscattering angles from these types of data. Again, long optical transmission paths are involved and the atmospheric transmission factor enters rather crucially into the instrumental calibration. Nephelometers, which measure the volume scattering function directly, obviate these difficulties. On the one hand the measurements are confined to a small volume of atmosphere, thereby precluding transmission path problems, and on the other the instrument can be calibrated in absolute quantities.

In England, Waldram (1954) used a polar nephelometer aboard an aircraft—and later on a tethered balloon—to determined $\beta(\phi)$ as a function of altitude up to 9 km. In Australia, Crosby and Koerber (1962) made measurements with a balloon-borne integrating nephelometer up to around 3 km. Although nephelometry is widely used in ground-based experiments, high altitude measurements of $\beta(\phi)$ have generally not been attempted due to instrumentation difficulties. However, with the advent of intense light sources that are operable in this extreme environment, a balloon-borne polar nephelometer presents itself as an ideal instrument for making quantitative atmospheric optics measurements.

Under contract from AFCRL, Spectra Metrics, Inc., Burlington, Massachusetts, designed a modified polar nephelometer, with detectors fixed at five scattering angles, for high-altitude balloon measurements. From November 1967 to November 1969, a series of experiments was conducted to altitudes of approximately 21 km with limited success. In view of the small concentrations of aerosol particles (perhaps 0.02 cm^{-3}) that can occur over the altitude profile, an instrument approximately 3 meters in diameter was required to provide a sufficiently large scattering volume. Notwithstanding the constructional problems this entails, the prime obstacle to reliable data apparently came from the use of a pulsed light source.

Since the pulse duration was 400 μsec and the detected signals were integrated over this interval, the noise bandwidth could not be limited—the two being inversely related. Furthermore, when observed for short time intervals, scattering by individual particles in the pulse volume is inherently noise-like. This results in signals that are not very meaningful statistically, particularly at the low signal levels concomitant with very low aerosol concentrations.

As an outgrowth of this effort, a nephelometer was constructed in-house at AFCRL with generally the same design concepts as the Spectra Metrics unit, but with some important modifications. The basic elements of the AFCRL-designed instrument are a xenon light source, operated CW, and five identical photometers mounted on a 3.3-m-diam octagonal gondola. The photometers measure the light scattering at 22°, 45°, 90°, 135°, and 157° from a volume of atmosphere (about 250 cm^3) defined by the intersection of the source and receiver beams. The source beam is modulated at 22.5 Hz and a.c. synchronous detection employed to restrict the noise bandwidth and thus provide a considerable improvement in the signal-to-noise ratio. The scattered light is detected at four wavelengths (4750 Å, 5150 Å, 6600 Å, and 7450 Å) with an S-20 photomultiplier in each photometer, and the data output was recorded in-flight on magnetic tape. To remove the restriction to nighttime operation—a limitation on most atmospheric scattering measurements in the visible spectral range—the gondola was designed in such a manner that sunlight was completely excluded from the measurement volume.

On November 3, 1970, at approximately 1155 hours, the nephelometer was flown to 26 km from White Sands Missile Range, New Mexico, as one of the subsystems under Project ATOM. This report gives the results of the flight and indicates the capabilities of the nephelometer approach for providing a good profile of the volume scattering function as a function of altitude, wavelength, and scattering angle. Moreover, the light polarization properties of atmospheric aerosols are shown to offer an excellent signature for the presence of dust layers, thus corroborating changes in scattering function occurring as a consequence of the aerosol contribution to the total scattering. Time lapse horizon photographs were also made during the flight, and these further verified the observations discerned from the nephelometer data.

2. THEORETICAL CONSIDERATIONS

A beam of unpolarized light with intensity E(Wcm^{-2}) incident on the scattering volume $V(\phi)$ produces a radiance at the scattering angle ϕ given by

$$I(\phi) = \beta(\phi)\, E\, V(\phi)\ (W\ sr^{-1}) \qquad (1)$$

where $\beta(\phi)$ is the angular volume scattering function ($cm^{-1}\ sr^{-1}$), $\beta(\phi)$ is simply the fraction of the incident light scattered by molecules and particles in the volume $V(\phi)$.

For a system in which the source and receiver are imaged at the scattering volume, the radiant power at the photometer entrance aperture of area A at a distance R from the scattering volume is

$$F(\phi) = \frac{\beta(\phi)\, E\, V(\phi)\, A}{R^2} \text{ (W)} . \tag{2}$$

Now $V(\phi)$ is defined by the intersection of the source beam and the detector field of view and, for a particular scattering angle, is fixed (see Figure 1). Similarly E, A, and R, as well as the transmittance of the receiver optics (lenses, filters, etc.), are design constants that in the actual experimental measurements are lumped together in a calibration factor for the instrument. As a result, if the instrumental response to received energy is linear the only remaining variable is $\beta(\phi)$ and the response can be expressed as

$$W(\phi_s) = K_1 \beta_\lambda(\phi_s) \tag{3}$$

where K_1 is the calibration factor for a photometer at scattering angle ϕ_s with a spectral filter of wavelength λ. This factor is determined, in absolute quantities, in the laboratory so that $\beta_\lambda(\phi_s)$ is ascertained absolutely from the recorded output data.

The angular distribution of the scattered light is usually expressed by the phase function, defined by

$$P(\phi) = \frac{\beta(\phi)}{2\pi \int_0^\pi \beta(\phi) \sin\phi d\phi} \text{ (sr}^{-1}\text{)}.$$

The integral in the denominator is the total scattering coefficient σ (cm^{-1}). Since air molecules and aerosols scatter the light independently, we may write the total scattering function as $\beta_\lambda(\phi_s) = \sigma_{r\lambda} P_r(\phi_s) + \sigma_{P\lambda} P_P(\phi_s)$ where $\sigma_{r\lambda}$ is the Rayleigh scattering coefficient (cm^{-1}), and $P_r(\phi_s)$ is the normalized Rayleigh phase function (sr^{-1}), $\sigma_{P\lambda}$ is the aerosol scattering coefficient (cm^{-1}), and $P_p(\phi_s)$ is the normalized aerosol phase function (sr^{-1}). The Rayleigh phase function is given by

$$P_r(\phi_s) = \frac{3}{16\pi}(1 + \cos^2\phi_s) . \tag{4}$$

Moreover, the Rayleigh scattering coefficient $\sigma_{r\lambda}$ is well known and given in the literature (Elterman, 1968). Thus in principle $\beta_\lambda(\phi_s)$ and thereby $\sigma_{P\lambda} P_P(\phi_s)$ can be determined from the response $W(\phi_s)$, once the factor K is determined from the instrument calibration.

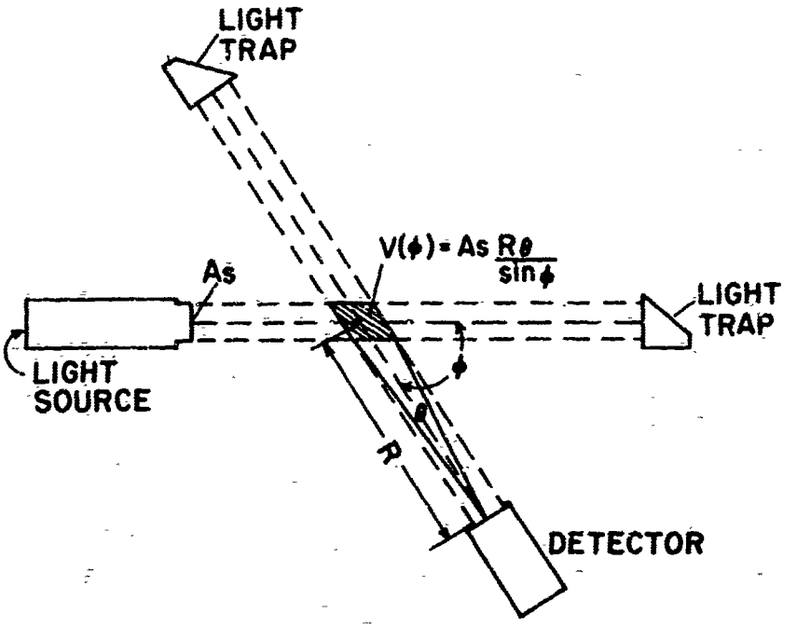

Figure 1. Scattering Volume Geometry

Equation (4) gives the Rayleigh-phase function for the total scattered light, which is simply one half the sum of the vertical and horizontal components of the light polarized by scattering from air molecules. The degree of polarization is given by (see for example, Born and Wolf, 1959)

$$P(\phi_s) = \frac{I_v - I_H}{I_v + I_H} = \frac{1-\cos^2\phi_s}{1+\cos^2\phi_s} = \frac{\sin^2\phi_s}{1+\cos^2\phi_s}, \qquad (5)$$

which predicts complete polarization at a scattering angle of 90^o, and suggests further that departures from it are attributable to non-Rayleigh scattering, that is, scattering from atmospheric dust or aerosols. One surmises, therefore, that if the ratio of the vertical and horizontal components of the scattered light is determined, it will provide a measure of the degree of polarization, a rather sensitive indicator of aerosol scattering.

Another parameter that serves as an indicator of atmospheric particulate matter is the forward-to-back scatter ratio. This follows from the fact that Rayleigh scattering is symmetrical about the 90^o scattering angle, as can be seen from an inspection of Eq. (4). For example, the phase function is the same for

scattering at 45° and 135°. The ratio of the 45° volume scattering function to the 135° volume scattering function should thus be unity for a pure Rayleigh atmosphere, and values greater than unity are a result of aerosol scattering. We have, therefore, three independent measurements—the volume scattering function, the polarization, and the forward-to-backscatter ratio—from which the vertical distribution of atmospheric aerosols can be ascertained.

3. CALIBRATION

A unique method for calibrating the polar nephelometer was developed by Pritchard and Elliott (1960). It entails comparing the intensity of the light scattered by the atmosphere with the intensity from a thin diffusing screen of known reflectance and transmittance. The screen is placed in the sample space, that is, the common volume, and the intensity of the light reflected or transmitted is then recorded as the screen is moved through the volume. This results in a curve characteristic of the source-receiver beam geometry at a given scattering angle; the area under the curve provides the calibration factor for determining the intensity of the light scattered by an atmospheric sample under the same conditions of angle and wavelength. Figure 2 shows a typical curve.

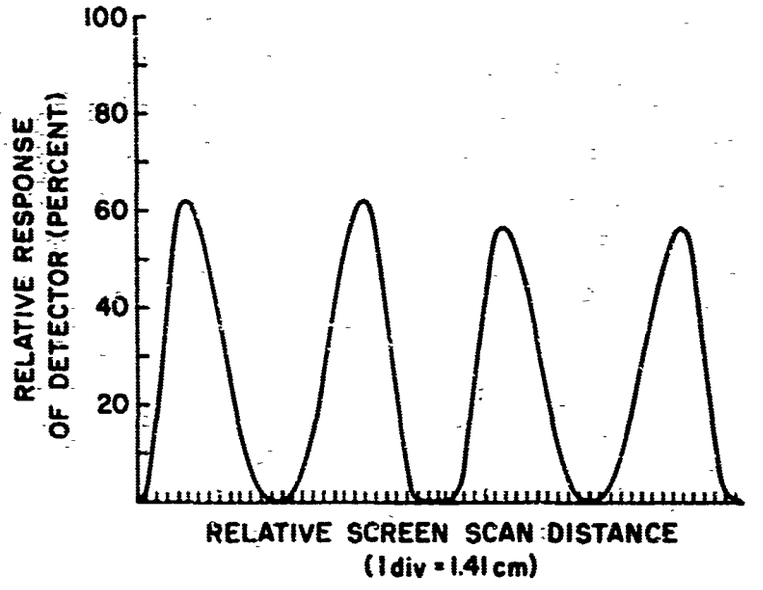

Figure 2. Calibration Curve for 7450 Å (V) and 7450 Å (H) at 135°, Reading Left to Right. Forward and backward traversals of the screen are shown

Since proof of this calibration technique is given by Pritchard and Elliot, it is only necessary to state the result here. It is shown that the volume scattering function in absolute quantities is given by

$$\beta = \frac{R\cos\gamma' \cos\gamma'' W_a}{\pi \int W_c dx} \quad [cm^{-1} sr^{-1}] \tag{6}$$

where R is the reflectance (for backscatter) or transmittance (for forward scatter), γ' is the angle of incidence of the transmitter beam, that is, the angle between the normal to the screen and the transmitter axis, γ'' is the angle between the normal to the screen and the receiver axis, $\int W_c dx$ is the recorded integral referred to above, and W_a is the instrumental response due to a volume of atmosphere. To compare Eq. (6) with Eq. (3), we see that $W_a = W(\phi_s)$ and the calibration factor of the instrument is

$$K = \frac{1}{K_1} = \frac{R\cos\gamma' \cos\gamma''}{\pi \int W_c dx} . \tag{7}$$

(In the particular nephelometer configuration used, $\gamma' = \gamma'' = \phi_s/2$.)

The salient feature of the calibration technique is that it requires no assumptions regarding sampling volume, uniformity of illumination, or equipment sensitivity. However, optical attenuators used to reduce the source intensity during the nephelometer calibration can introduce systematic errors if their attenuation is not measured precisely. Finally, once the value of K is determined as a function of scattering angle and wavelength, the corresponding values of $\beta(\phi_s)$ are calculable, in absolute value, from the instrumental response by using Eq. (3).

4. INSTRUMENTATION

A diagram of the nephelometer configuration is shown in Figure 3. An unpolarized 150-W xenon light source manufactured by ILC Corporation provides a uniformly illuminated project area 5.7-cm square at the center of the instrument. The source was operated CW, but chopped at 22.5 Hz to give intensity modulation and thereby allow synchronous detection as a means of suppressing unwanted signals.

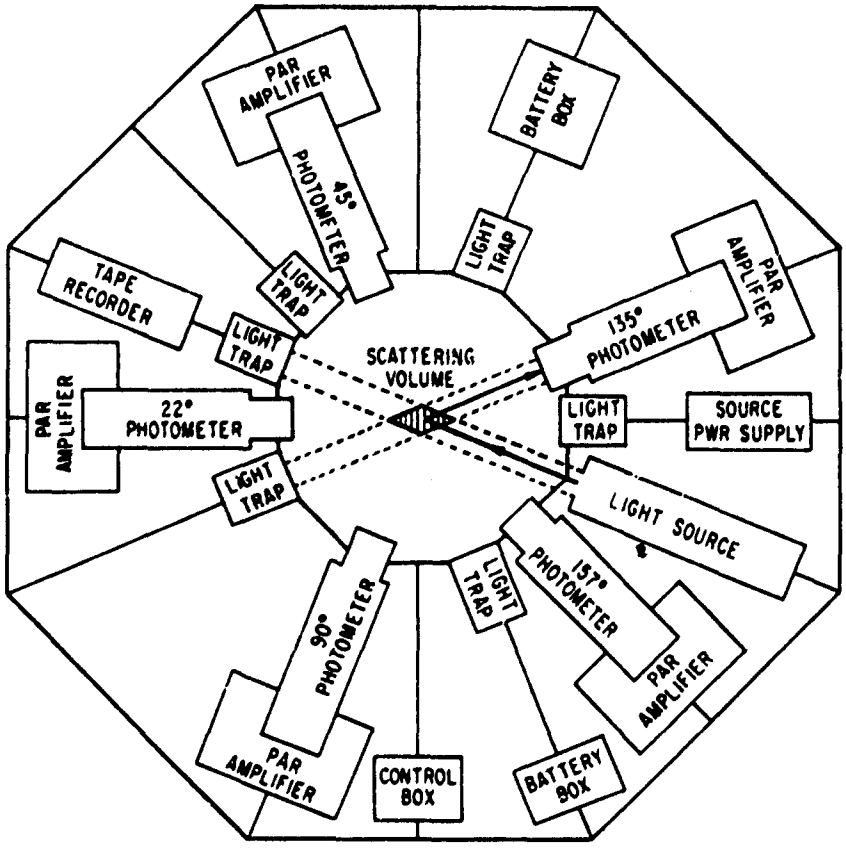

Figure 3. Balloon-borne Nephelometer Schematic

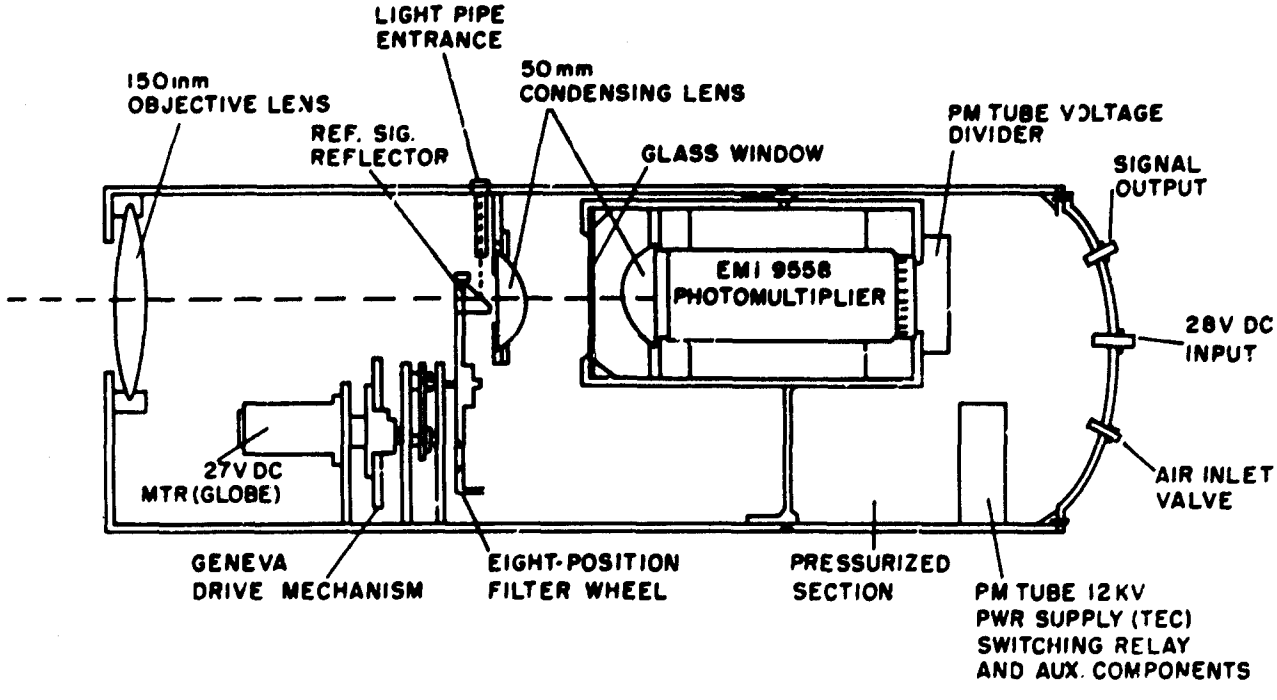

Figure 4. Typical Photometer Design

The typical receiving photometer is essentially a telescope focused at the center of the instrument, approximately 69 cm from the objective lens. The optical configuration is shown in Figure 4. A 2.5-cm square aperture serves as the field stop and provides a field of view of about 6^{o}. This aperture is imaged by the objective lens, resulting in a 7.6-cm square acceptance area and thereby defining a transmitter-receiver common volume with dimensions of 5.7 cm × 5.7 cm × 7.6 cm when viewed at 90^{o}. A 7.6-cm square aperture is placed in front of the objective lens to further collimate the light received from the measurement volume and to accommodate the receiver solid angle with its field of view.

The objective lens focuses the scattered light on the field stop. A pair of aspheric condenser lenses behind the stop images the objective lens onto an EMI 9558 photomultiplier having an S-20 spectral response. This optical configuration gives a sharply defined sensitivity profile across the beam in the region of intersection with the source beam, and also provides essentially uniform sensitivity throughout the common value.

An eight-position filter wheel is mounted adjacent to the square-field aperture. Spectral filters at four wavelengths (4750 Å, 5150 Å, 6600 Å, and 7450 Å with 1/2 bandwidth ± 110 Å) are used and the filter wheel is advanced via a Geneva drive mechanism at a rate of 10 rpm, thus providing a sampling rate of nearly 0.7 sec per filter. For the balloon flight the 4750 Å and the 7450 Å filters had linear polarizers laminated to their surfaces so that the vertical and horizontal polarization of the scattered light could be analyzed sequentially at these wavelengths. The remaining two positions on the filter wheel were used to check the zero level, that is, the scattered light was blocked, and to provide a reference signal directly from the source (via light pipes) to monitor the source intensity as well as gain changes in the photometer.

The photomultiplier output is fed to a Princeton Applied Research (PAR) Model 120 Lock-In Amplifier that is fixed-tuned to the 22.5-Hz chopper frequency. This provided ample sensitivity and noise suppression. An Ampex Model AR214, 14-track magnetic-tape recorder is used to store the data output from each receiver unit. In order to cover the wide dynamic range of signals detected over the flight profile, the PM tubes were operated at reduced sensitivity for the first 9 Km, and the output from each amplifier was recorded at two tape recorder gain settings—one greater than the other by a factor of 10.

Light traps are located opposite the source and each photometer in order to reduce the amount of stray radiation seen by the observation beams and to provide a black background beyond the measurement volume. An optical schematic of a light trap is shown in Figure 5. Light entering the trap is incident at 45^{o} upon a black specularly reflecting plexiglass surface. Most of the light is absorbed by the first surface; the specularly reflected component strikes a second plate, which is oriented at a slight angle with respect to the first and is

directed further into the trap where it is absorbed during many additional reflections. The only light leaving the trap—if it is clean and dust free—is negligible ($\sim 6 \times 10^{-6}$), due to non-specular reflection from the first surface. For the balloon flight, however, only one plexiglass light trap was used, opposite the source; the other traps were simply lined with black velvet.

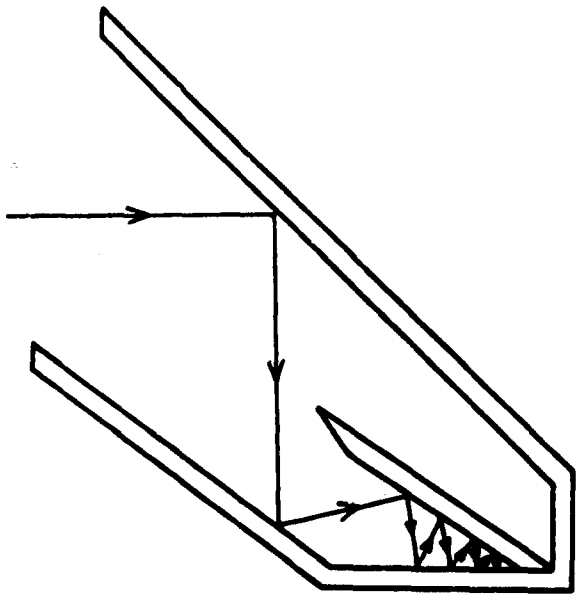

Figure 5. Light Trap

A rather critical consideration in overall nephelometer design is a gondola housing structure that prevents sunlight from reaching the scattering volume and at the same time allows a free-flow of atmosphere so as not to disturb the measurement volume. This was accomplished by mounting the equipment on a 3.3-m-diam octagonal frame, fabricated from aluminum U-channel beams, and building a concentric housing structure of highly reflecting aluminum sheets. The resulting octagonal "doughnut" was 0.6-m high with a 1-m-diam center section. At the top and bottom of the center section, removable sunlight baffles provide adequate sun shielding as well as entrance and exit ducts through which the ambient aerosols can flow unobstructed.

5. EXPERIMENTAL OBSERVATIONS AND RESULTS

The high altitude balloon (2 million cu ft) that carried the experimental payload was launched from the Stallion Range Center, WSMR, at 1155 MST on 3 November 1970 into a clear sky. The gondola landed 4 hr, 22 min later, 200 miles eastward near the New Mexico-Texas border. Figure 6 shows the flight trajectory. The payload reached better than 26-km altitude and was recovered intact, with no damage to the equipment.

Although this was the maiden balloon flight for the instrument, with all the "bugs" and unforeseen difficulties accompanying it, some rather interesting and meaningful results were obtained.

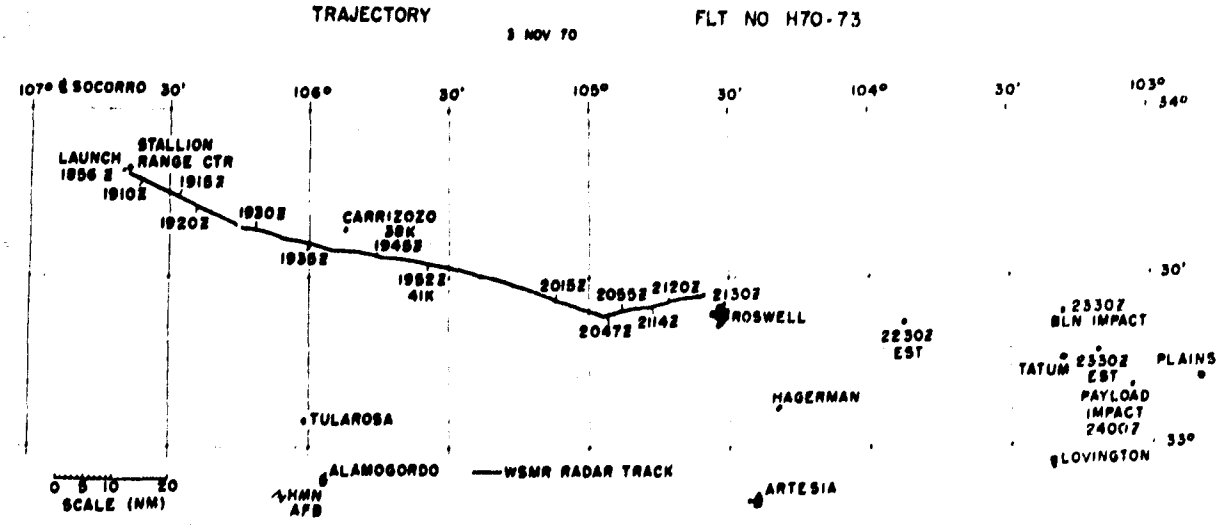

Figure 6. Flight Trajectory

As aforementioned, the data output from each receiver unit was recorded in flight on magnetic tape. Unfortunately, the playback contained readable outputs from only the photometers at 45°, 90°, and 135°, and of these the 135° unit ceased operation at around 15 km when the filter-wheel drive mechanism jammed. The recorded signal amplitudes were averaged over 13 or so data points, which corresponds to flight time intervals of about 1.2 min. Since the rate of rise of the balloon was 600 ft/min, this implies an altitude interval of about 0.2 km. The amplitudes were expressed in terms of analog voltage outputs from the respective PAR amplifiers. These voltages were used in conjunction with the pre-flight calibration factors for each photometer and spectral filter to calculate the volume scattering function as a function of altitude.

Figures 7 through Figure 15 show the flight results for the three scattering angles and four wavelengths. In addition, the appropriate Rayleigh profiles are plotted to provide a measure of the contribution of atmospheric aerosols to the total scattering function. Indeed, it is revealing that there was no pure Rayleigh scattering over the entire flight, although the 4750 Å and 5150 Å scattering follow the Rayleigh slope more closely than the longer wavelengths. Moreover, the vertically polarized 4750 Å at 90° is the least sensitive to the presence of aerosols, which corroborates the assertion that the air molecules polarize the incident light and should be more pronounced at the shortest wavelength due to the λ^{-4} Rayleigh intensity factor. On the other hand, the horizontal component is quite sensitive to aerosols in the scattering volume, since the 90° Rayleigh component is theoretically zero. At 45° the polarization is less, thus the aerosol influence is dominant at all wavelengths for that angle.

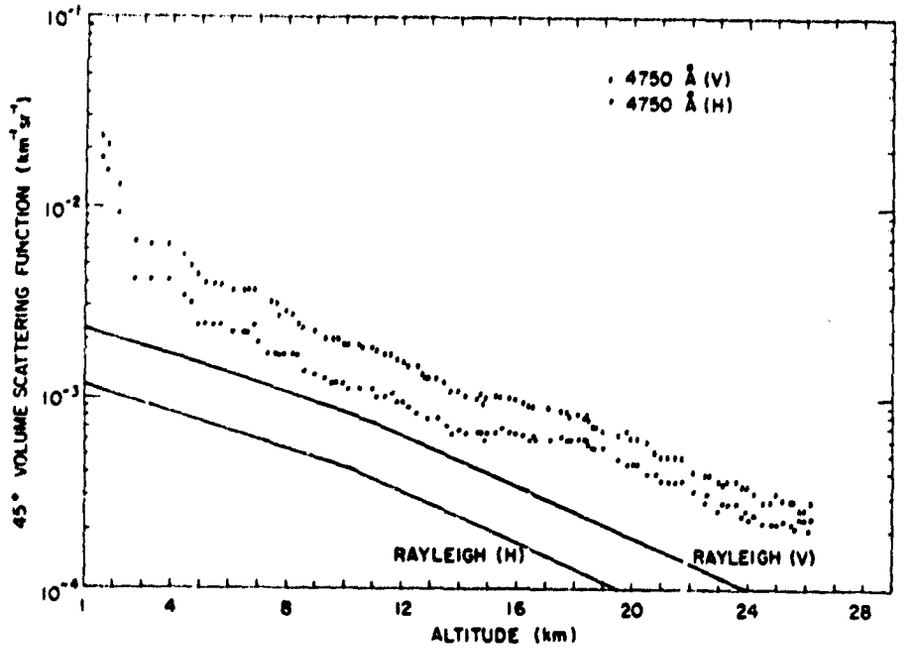

Figure 7. 45° Volume Scattering Function vs Altitude at 4750 Å (V) and 4750 Å (H)

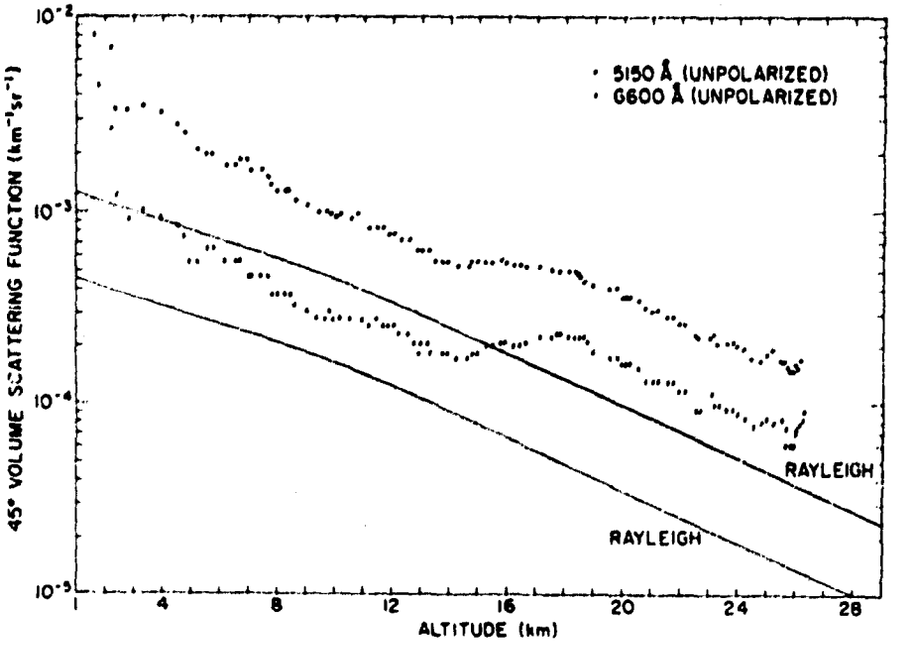

Figure 8. 45° Volume Scattering Function vs Altitude at 5150 Å and 6600 Å

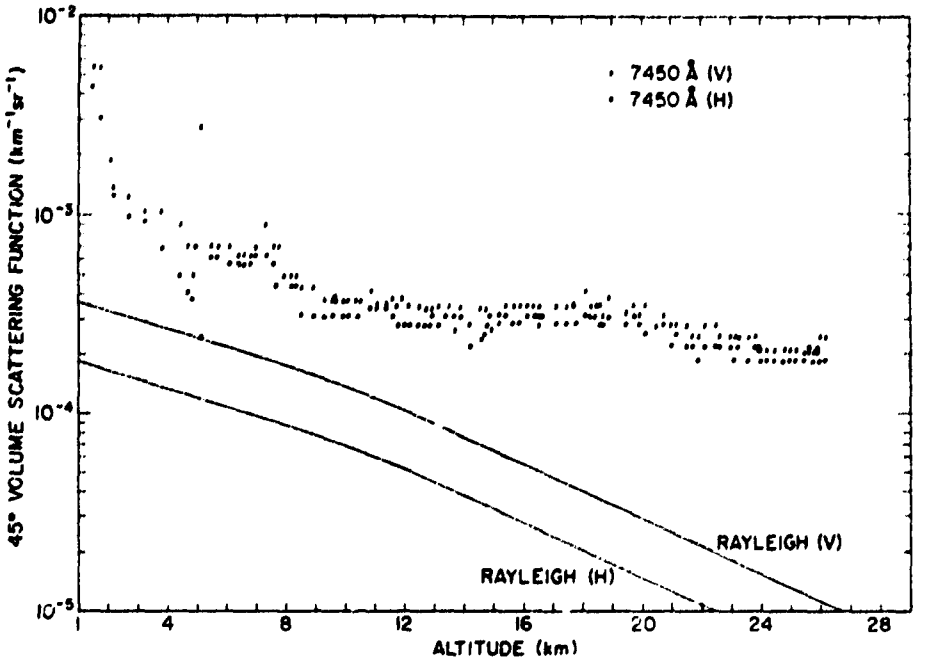

Figure 9. 45° Volume Scattering Function vs Altitude at 7450 Å (V) and 7450 Å (H)

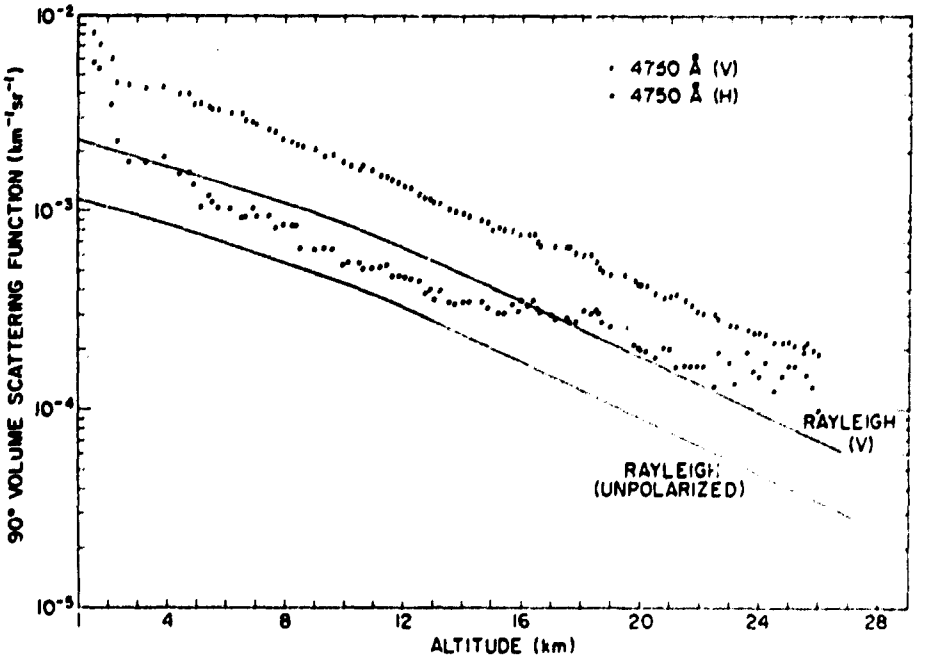

Figure 10. 90° Volume Scattering Function vs Altitude at 4750 Å (V) and 4750 Å (H)

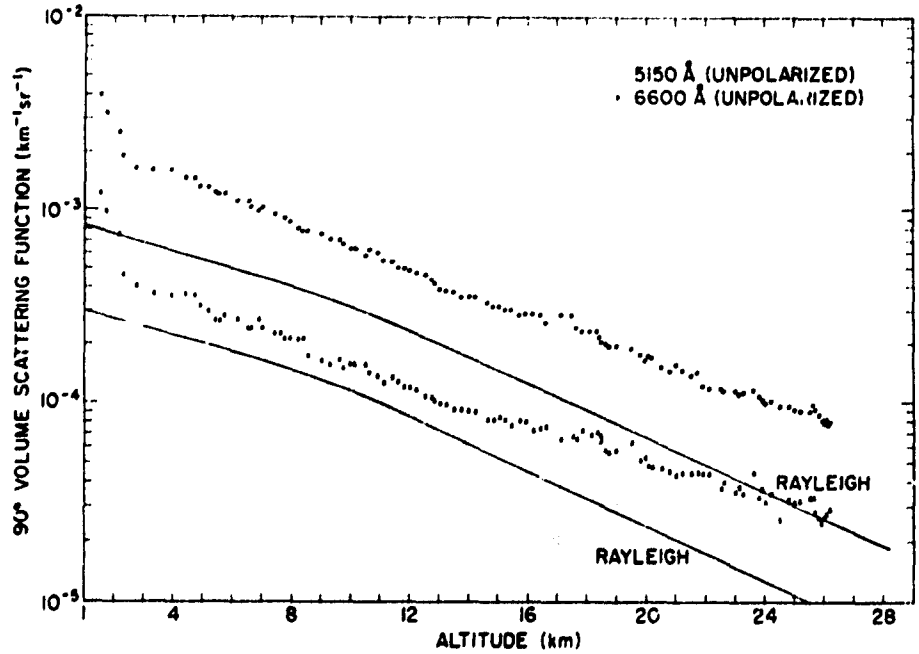

Figure 11. 90° Volume Scattering Function vs Altitude at 5150 Å and 6600 Å

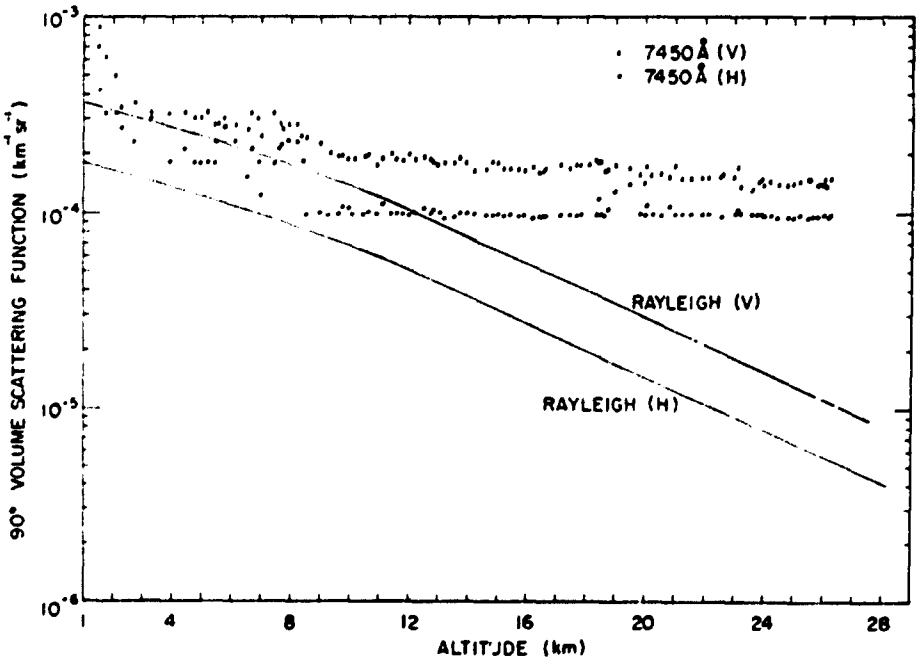

Figure 12. 90° Volume Scattering Function vs Altitude at 7450 Å (V) and 7450 Å (H)

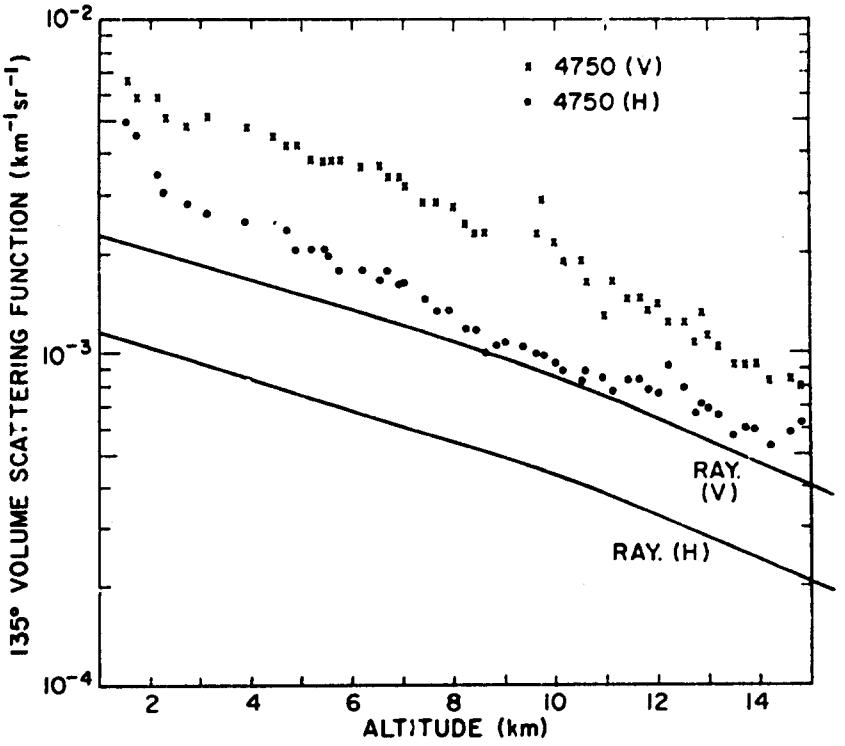

Figure 13. 135° Volume Scattering Function vs Altitude at 4750 Å (V) and 4750 Å (H)

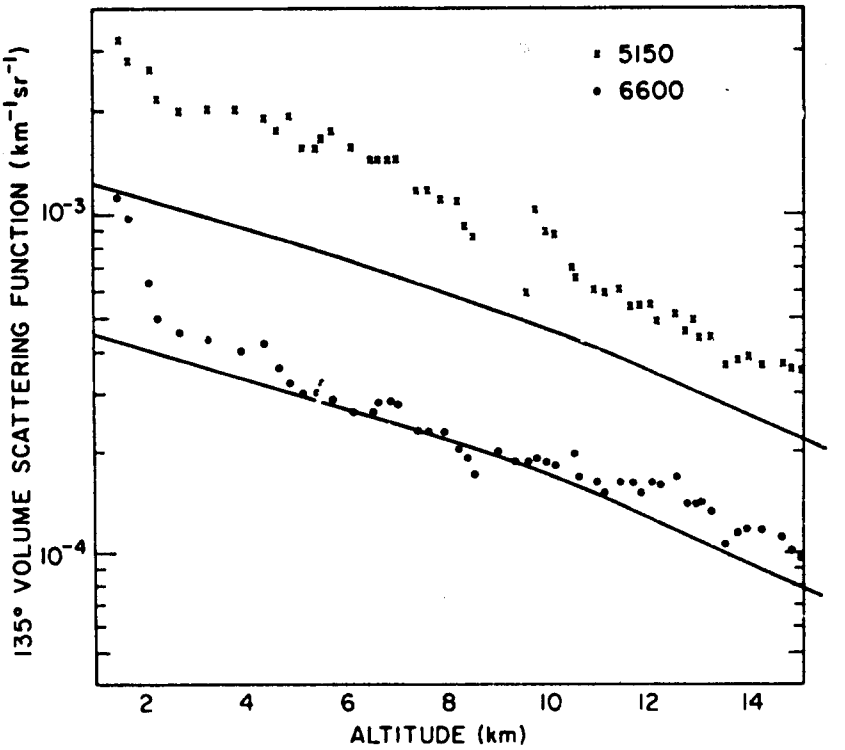

Figure 14. 135° Volume Scattering Function vs Altitude at 5150 Å and 6600 Å

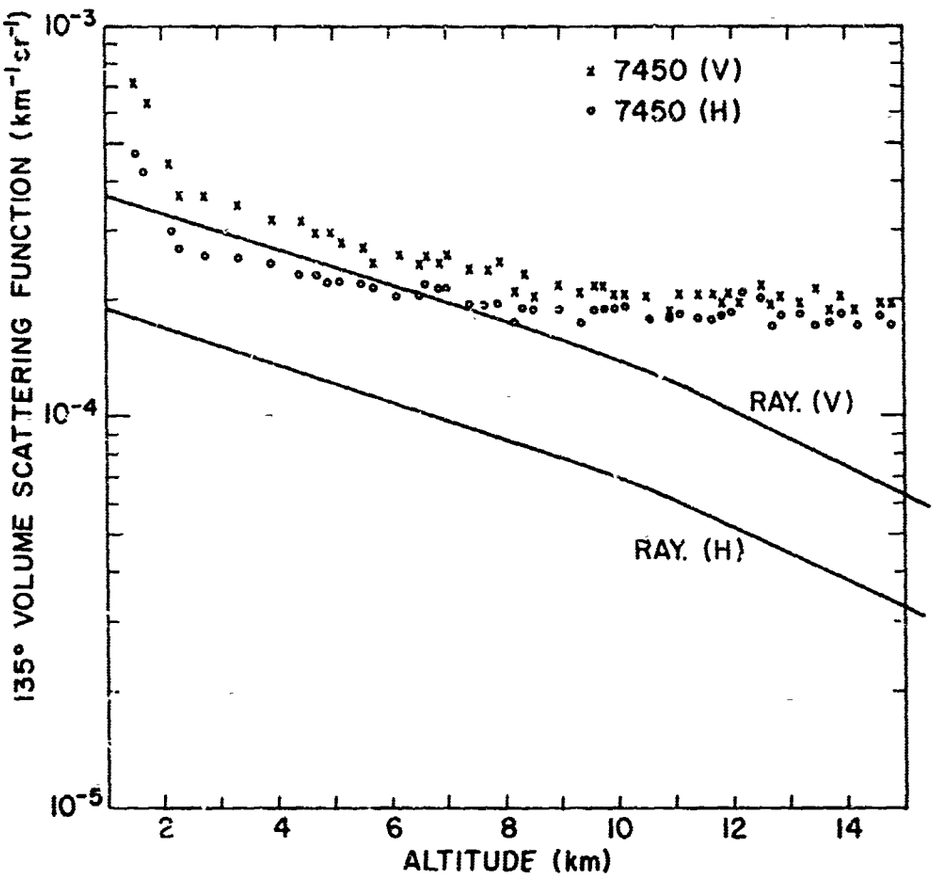

Figure 15. 135° Volume Scattering Function vs Altitude × 7450 Å(V) and ⊙ 7450 Å(H)

The values of the volume scattering functions follow the expected pattern. That is, they are greater in the forward direction, when particulate matter is present, and the increase is further biased toward the longer wavelengths. The 7450 Å scattering is seen to be influenced almost completely by aerosols. Unfortunately, however, due to equipment malfunctions, a vertical profile of the scattering phase function could be drawn for only three points (at 45°, 90°, and 135°). Nevertheless, Figures 16a to 16d reveal, at least qualitatively, how the angular dependence of the scattering function changes with aerosol concentration.

The polarization ratio I_V/I_H as a function of altitude is plotted in Figures 17 and 18 for the 4750 Å wavelength, at 45° and 90° respectively. These figures show the rather striking role that aerosols play in affecting the polarization of the

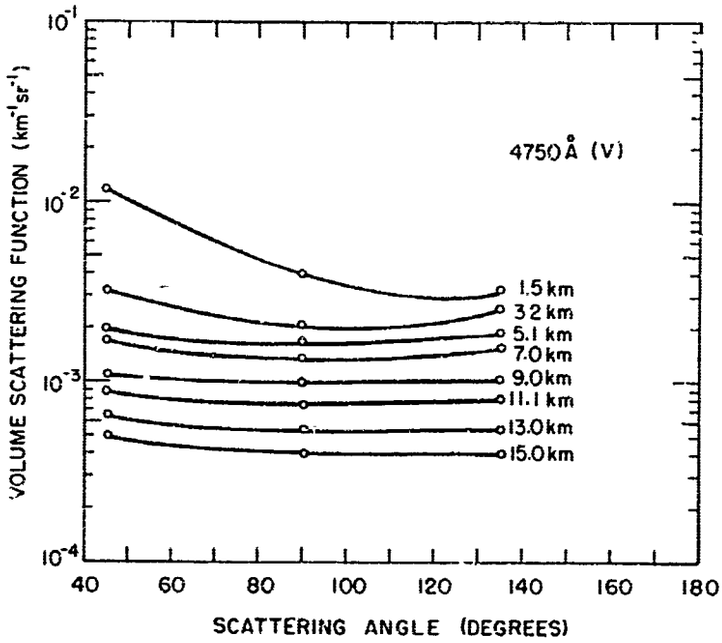

Figure 16a. Volume Scattering Function vs Scattering Angle at 4750 Å (V)

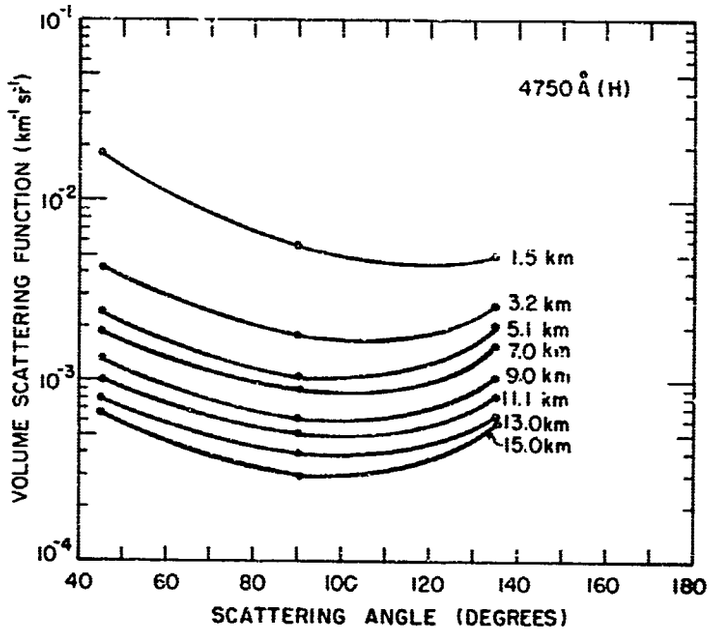

Figure 16b. Volume Scattering Function vs Scattering Angle at 4750 Å (H)

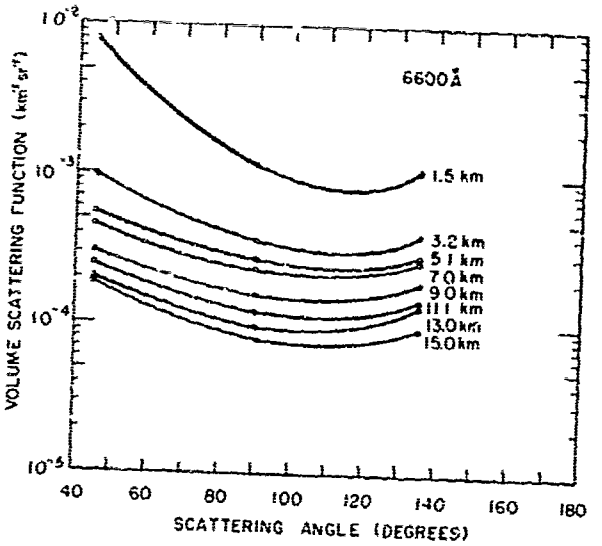

Figure 16c. Volume Scattering Function vs Scattering Angle at 6600 Å (unpolarized)

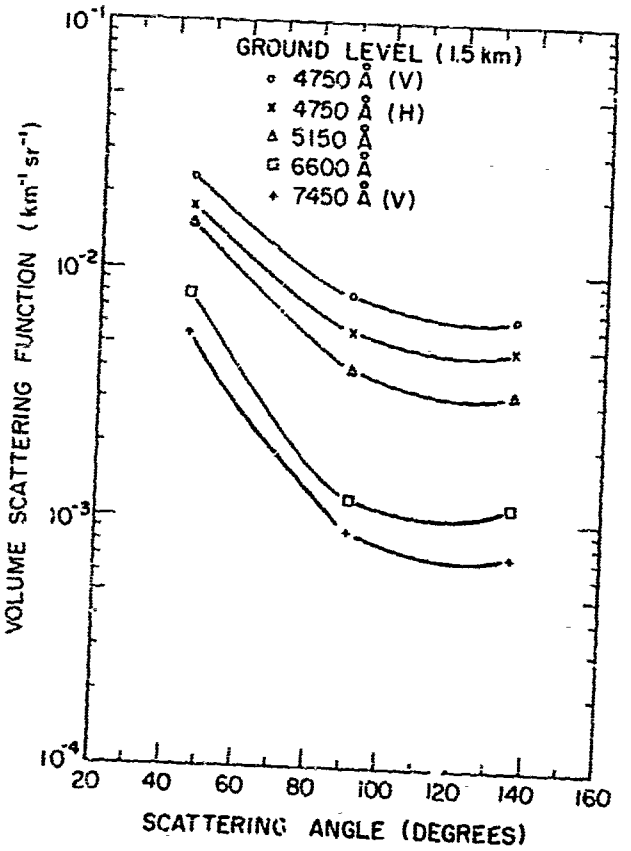

Figure 16d. Volume Scattering Function vs Scattering Angle at Ground Level for Four Wavelengths

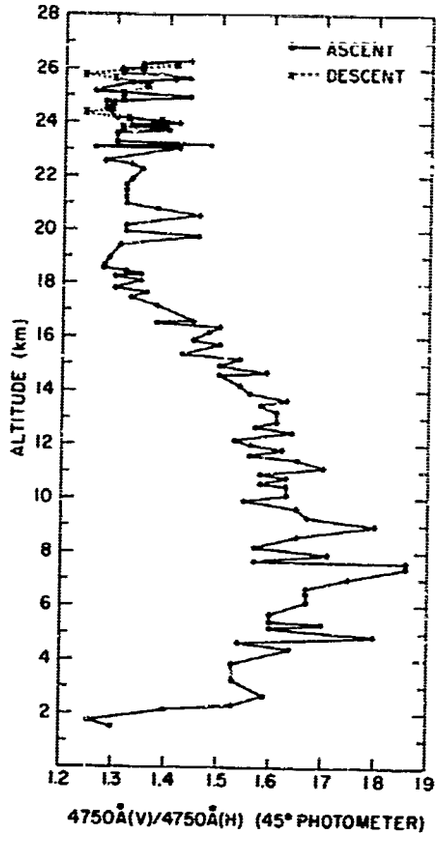

Figure 17. 45° Polarization Ratio, I_V/I_H vs Altitude at 4750 Å

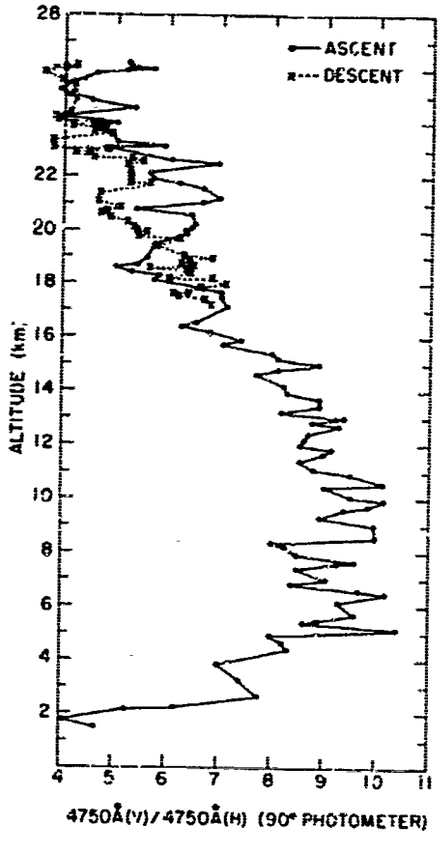

Figure 18. 90° Polarization Ratio, I_V/I_H vs Altitude at 4750 Å

scattered light, the degree of polarization varying inversely with the aerosol number density or turbidity. For example, at 90° an I_V/I_H value of 10 means that the unpolarized incident beam became 82 percent polarized upon scattering, and a ratio of 4 indicates that it became 60 percent polarized. The dominance of the molecular contribution to the polarization of the scattered light is apparent. However, at 45° it varies from about 20 percent in the relatively clear air to 13 percent when the aerosol concentration is greatest. Even though the polarization is reduced at 45°, as Eq. (5) predicts, the two profiles have much the same structure and the values compare favorably with those of Bullrich (1964).

Figure 19 shows the ratio of the scattering function at 45° to that of 135° from ground to 15 km, and reveals marked variations as the aerosol concentration changes. Moreover, the ratio varies with wavelength and the scattering at the longer wavelengths is stronger in the forward direction, as is clearly evident from the plots.

In comparing all the figures in order to get a composite picture, one finds some common structure in the profiles. After passing through the ground-level dust (the visibility was better than 30 km), some aerosol fine structure was evident at 4-, 5.7-, and 7.5-km altitude. Noteworthy is the increase in the forward-to-backscatter ratio at these altitudes.

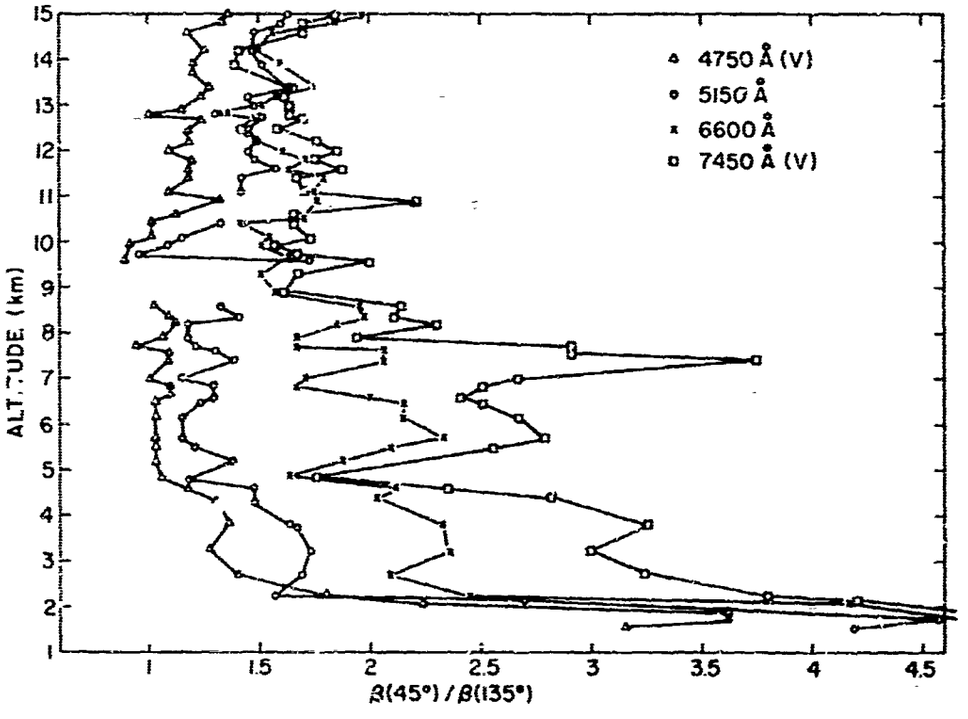

Figure 19. Forward-to-Backscatter Ratio vs Altitude and Wavelength

This aerosol structuring appears to be closely correlated with changes in ambient temperature and lapse rate (See Figure 20 for the flight profile). In fact, the presence of a double tropopause on the day of the flight—a not uncommon phenomena in the launch vicinity—can be verified from the nephelometer data. Near the second tropopause at 15 km (temperature -68°C), the particle concentration begins to increase appreciably, and the first of the well-known stratospheric dust layers emerges at 17 km, reaching a maximum at about 18.5 km. This is particularly well defined in the polarization profiles. Of special note is the fact that the polarization from the stratospheric dust is approximately the same as that due to the ground-level particles on the "clear" day of the flight. This implies the size distributions should be comparable.

At least four other stratospheric layers were prominently manifested during the balloon ascent. Their altitudes were ascertained from a mean of the separate profiles. A layer at about 21 km appears in all the profiles as well as one between 23 and 24 km with maximum concentration at about 23.8 km. In addition, the polarization data and the 45° scattering functions indicate a layer at 25 km and a somewhat weaker one at 26 km. On the descent phase of the flight, the 26-km layer was stronger and the 25-km layer had apparently moved to 24 km or so. The 23-km layer was not sharply defined, but the one at 21 km was broader than it was on the up-leg of the flight. The layer at 18.5 km was still present on descent.

Horizon time-lapse color photographs taken with a camera mounted on top of the gondola as an independent experimental payload showed much the same aerosol structure in the stratosphere as that measured with the nephelometer (Volz, 1971). The stratospheric dust has been the subject of numerous investigations—Junge et al (1961), Volz and Goody (1962), and Rosen (1968) among several others—and has been observed by researchers in all parts of the world.

The observed correlation between aerosol concentration and temperature profile has been reported by other researchers (Elterman et al, 1969; McCormick, 1970), and is logically explained by atmospheric processes. Since the flight was at noon, particles were convected upwards due to warming at the earth's surface; thus, the lower altitude fine structure emerges as a result of the convective-mixing process. However, at a temperature inversion this upward transport is inhibited and a turbidity maximum results. The observed aerosol layer with maximum concentration at 7.5 km is then interpreted as resulting from the combined effects of the surface convective layer and a weak tropopause. This aerosol structure is apparent in both the polarization profiles and the plots of forward-to-backscatter ratio.

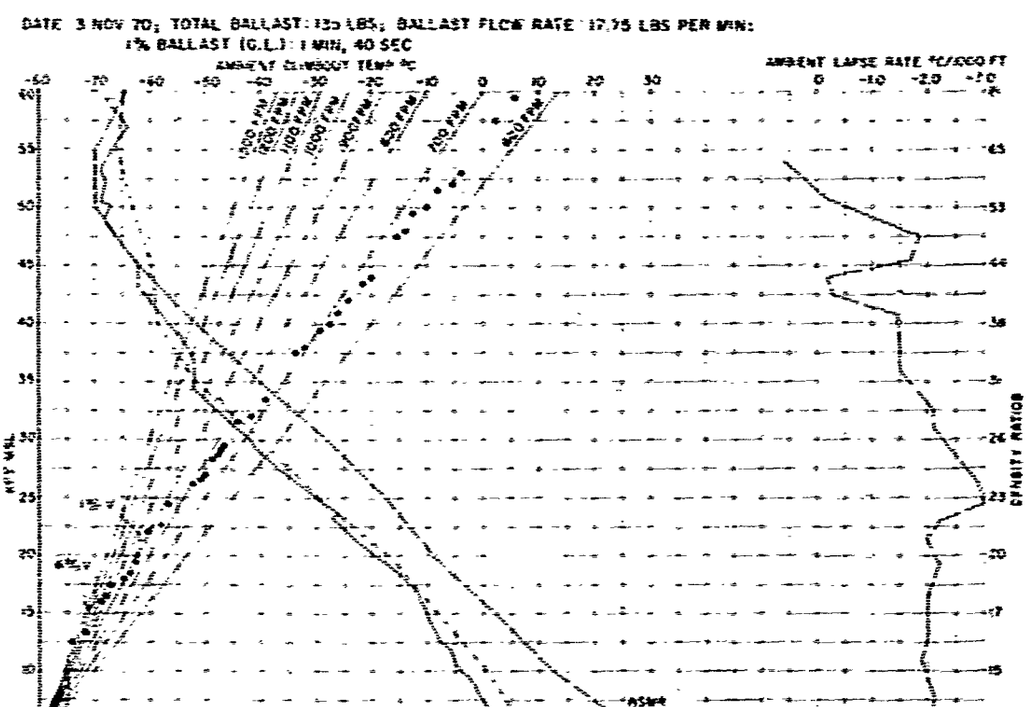

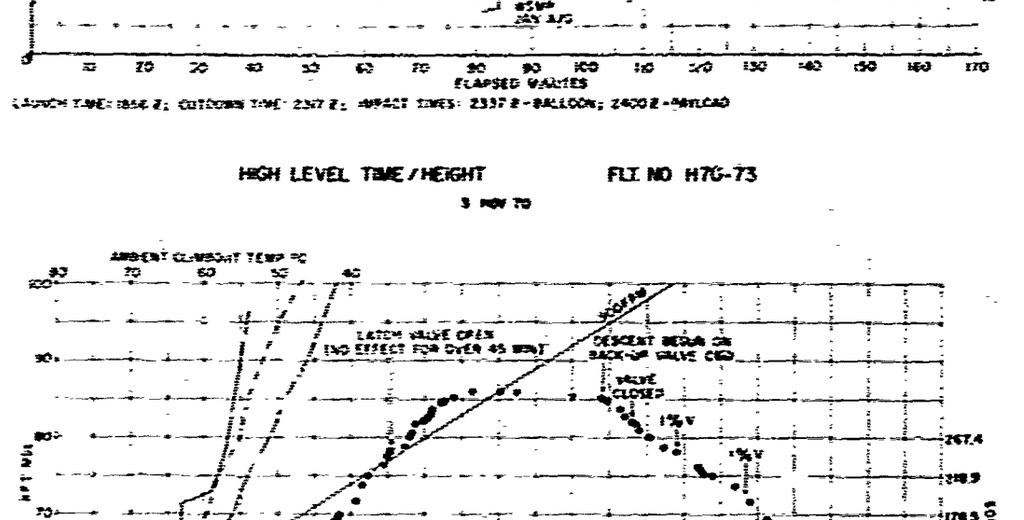

Figure 20. Balloon Flight Profile

The stratospheric aerosol is also associated with the onset of a tropopause; indeed, the primary tropopause, often designated the tropical tropopause, is almost invariably characterized by a turbidity maximum. This tropopause is much more stable, however, and volcanic dust that is transported vertically by the intense convective activity in the tropical and subtropical regions remains in the stratosphere for years. Moreover, the air containing the aerosols undergoes advection, which produces the dust stratification usually observed.

6. CONCLUSIONS

The results from the balloon flight should be viewed as preliminary in the sense that they represent about a third of the data-acquisition capabilities of the nephelometer system. Nevertheless, the utility of such an instrument is quite apparent. It was possible to generate profiles of the volume scattering function versus altitude for three scattering angles and four wavelengths. Although a careful error analysis was not undertaken (the neutral density filters and optical attenuators used in calibration were the most likely source of error and would cause a constant bias in the volume scattering functions away from or toward the Rayleigh values), perhaps at most a 20 percent error could be attributed to the calibration. The polarization profiles, however, are independent of the calibration since they were obtained by taking the ratio of two analog signals at the same wavelength, detected about 0.5 sec apart, with the same receiver. Similarly, the forward-to-backscatter ratio is less prone to calibration influences as these tend to divide out, particularly over a range of values for this ratio. In subsequent balloon flights the possible calibration errors can be reduced appreciably by carefully standardizing the optical components used. Other operational problems are remediable with minor equipment modifications.

Even though the amount of data was limited, there was sufficient information to show that the polar nephelometer is a very sensitive instrument for atmospheric optics investigations. Indeed, much more quantitative results than presented here can be discerned from the angular scattering of light and its dependence on wavelength and polarization. If, for example, the phase function is determined, the turbidity can be calculated from the polarization data, since an explicit relationship can be established between the two. From the wavelength dependence, there is a possible inference relative to particle sizes or at least size distribution.

The daytime operational capability of the balloon-borne polar nephelometer is an invaluable asset. This permits atmospheric optics measurements heretofore very difficult if not impossible to obtain. There is at present little information on the diurnal and nocturnal changes in the atmospheric aerosol structure, especially

in the troposphere. Since the convective phenomena play a major part in determining this structure, the importance of making observations during the day as well as night is thus obvious.

Acknowledgments

The authors would like to acknowledge the assistance of Carl Rust, Walter Jackson, Jack Halsel and the AFCRL machine shop personnel in the design and construction of the experimental package. Appreciation is also extended to Robert D. Maher, Michael F. Daddario, Dr. Frederick E. Volz, and John D. Essex for their invaluable help in the field and in the data reduction. The AFCRL balloon group at Holloman AFB, New Mexico, is commended for the successful flight and recovery of the equipment. Helpful reviews and discussions of the report were held with Dr. Robert W. Fenn.

References

Born, M., and Wolf, E. (1959) Principles of Optics. Pergamon Press, New York, p. 656

Bullrich, K. (1964) Scattered radiation in the atmosphere and the natural aerosol, from Adv. in Geophysics 10:101-257, H.E. Landsberg and J.E. Mieghem, Editors, Academic Press, N.Y.

Clemesha, B.R., Kent, G.S., and Wright, R.W. (1967) A laser radar for atmospheric studies, J. Appl. Meteorol. 6:386-395.

Collis, R.T.H., and Ligda, M.G.H. (1966) Note on lidar observations of particulate matter in the stratosphere, J. Atmos. Sci. 23:255-257.

Crosby, P., and Koerber, B.W. (1962) Scattering of light in the lower atmosphere, J. Opt. Soc. Am. 52:358-361.

Elterman, L. (1966) Aerosol measurements in the troposphere and stratosphere, Appl. Opt. 5:1769-1775.

Elterman, L. (1968) U.V., Visible and IR Attenuation for Altitudes to 50 Km, 1968, Report AFCRL-68-0153, AFCRL, Bedford, Mass.

Elterman, L., Wexler, R., and Chang, D.T. (1969) Features of tropospheric and stratospheric dust, Appl. Opt. 8:893-903.

Grams, G., and Fiocco, G. (1967) Stratospheric aerosol layer during 1964 and 1965, J. Geophys. Res. 72:3523-3542.

Junge, C.E., Chagnon, C.W., and Manson, J.E. (1961) Stratospheric aerosols, J. Meteorol. 18:81.

McCormick, M.P. (1970) Simultaneous multiple wavelength laser radar measurements of the lower atmosphere. Paper presented at Electro-Optics Systems Design Conference, New York.

References

Pritchard, E.S., and Elliott, W.G. (1960) Two instruments for atmospheric optics measurements, J. Opt. Soc. Am. 50:191-202.

Rosen, J. (1965) Simultaneous dust and ozone soundings over North and Central America, J. Geophys. Res. 73:479.

Volz, F.E. (1971)Stratospheric aerosol layers from balloon-borne horizon photographs. Paper in preparation.

Volz, F.E., and Coody, R.M. (1962) The intensity of the twilight and upper atmospheric dust, J. Atmos. Sci. 19:385-426.

Waldram, J.M. (1945) Measurements of the photometric properties of the upper atmosphere, J. Meteorol. 71:319-336.